

# Physical and Dynamical Linkages Between Lightning Jumps and Storm Conceptual Models

Christopher J. Schultz<sup>1,2,\*</sup>, Lawrence D. Carey<sup>2</sup>, Elise V. Schultz<sup>3</sup>, Richard J. Blakeslee<sup>1</sup> and Steven J. Goodman<sup>4</sup>

1. NASA Marshall Space Flight Center, Huntsville, AL, United States

2. Department of Atmospheric Science, University of Alabama-Huntsville, Huntsville, AL, United States

3. Earth System Science Center, University of Alabama-Huntsville, Huntsville, AL, United States

4. NOAA/NESDIS, Greenbelt, MD, United States

**ABSTRACT:** The presence and rates of total lightning are both correlated to and physically dependent upon storm updraft strength, mixed phase precipitation volume and the size of the charging zone. The updraft modulates the ingredients necessary for electrification within a thunderstorm, while the updraft also plays a critical role in the development of severe and hazardous weather. Therefore utilizing this relationship, the monitoring of lightning rates and jumps provides an additional piece of information on the evolution of a thunderstorm, more often than not, at higher temporal resolution than current operational radar systems. This correlation is the basis for the total lightning jump algorithm that has been developed in recent years.

Currently, the lightning jump algorithm is being tested in two separate but important efforts. Schultz et al. (2014; this conference) is exploring the transition of the algorithm from its research based formulation to a fully objective algorithm that includes storm tracking, Geostationary Lightning Mapper (GLM) Proxy data and the lightning jump algorithm. Chronis et al. (2014) provides context for the transition to current operational forecasting using lightning mapping array based products. However, what remains is an end-to-end physical and dynamical basis for coupling total lightning flash rates to severe storm manifestation, so the forecaster has a reason beyond simple correlation to utilize the lightning jump algorithm within their severe storm conceptual models.

Therefore, the physical basis for the lightning jump algorithm in relation to severe storm dynamics and microphysics is a key component that must be further explored. Many radar studies have examined flash rates and their relationship to updraft strength, updraft volume, precipitation-sized ice mass, etc.; however, their relationship specifically to lightning jumps is fragmented within the literature. Thus the goal of this study is to use multiple Doppler and polarimetric radar techniques to resolve the physical and dynamical storm characteristics specifically around the time of the lightning jump. This information will help forecasters anticipate lightning jump occurrence, or even be of use to determine future characteristics of a given storm (e.g., development of a mesocyclone, downdraft, or hail signature on radar), providing additional lead time/confidence in the severe storm warning paradigm.

---

\* Contact information: Christopher J. Schultz, NASA MSFC/UAH, 320 Sparkman Dr. Huntsville, AL, 35801, United States email: christopher.j.schultz@nasa.gov

## INTRODUCTION

The purpose of the total lightning jump algorithm (LJA) is to provide forecasters with an additional tool to identify potentially hazardous thunderstorms, yielding increased confidence in decisions within the operational warning environment. The LJA was first developed to objectively identify rapid increases in total lightning (also termed “lightning jumps”) that occur prior to the observance of severe and hazardous weather (Williams et al. 1999, Schultz et al. 2009, Gatlin and Goodman 2010, Schultz et al. 2011). However, a physical and kinematic framework leading up to and through the time of a lightning jump is still lacking within the literature. Many studies infer that there is a large increase in the updraft prior to or during the jump, but are not specific on what properties of the updraft are indeed increasing (e.g., maximum updraft speed vs volume or both) likely because these properties were not specifically observed. Therefore, the purpose of this work is to physically associate lightning jump occurrence to polarimetric and multi-Doppler radar measured thunderstorm intensity metrics and severe weather occurrence, thus providing a conceptual model that can be used to adapt the LJA to current operations.

## DATA AND METHODOLOGY

This study takes advantage of multiple observational platforms through the use of a well-established polarimetric, multiple Doppler domain and total lightning observations in North Central Alabama (Fig. 1). These unique observations allow for three dimensional (3D) retrievals of velocity and total lightning mapping. Furthermore, polarimetric radar information particle identification provides the volumetric growth/decay of precipitation sized ice (e.g., graupel, ice crystals) necessary for electrification.

One of the primary radars used in this analysis is the University of Alabama in Huntsville’s Advanced Radar for Meteorological and Operational Research (ARMOR; Schultz et al. 2012, Knupp et al. 2014). ARMOR is a C-band, polarimetric radar located at the Huntsville International Airport (KHSV). ARMOR operates in simultaneous linear transmit and receive (also known as slant 45), and collects horizontal reflectivity ( $Z_{HH}$ ), radial velocity ( $V_r$ ), spectrum width (SW), differential reflectivity ( $Z_{DR}$ ), correlation coefficient ( $\rho_{hv}$ ), and differential propagation phase ( $\Phi_{dp}$ ).

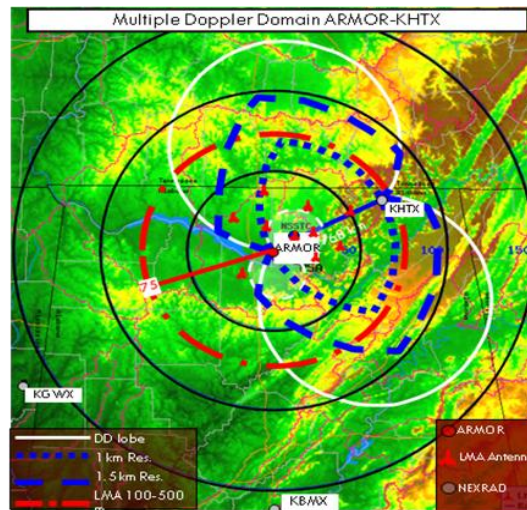


Figure 1. ARMOR-KHTX dual-Doppler domain (blue outline) and NALMA antenna locations (red markers)

Radar data were corrected for attenuation and differential attenuation (Bringi et al. 2001), and aliased velocities were unfolded using NCAR's SOLO3. Data were then gridded to a Cartesian coordinate system with a Cressman weighting scheme on a grid size of 300 x 300 x 19 using a resolution of 1 km x 1 km x 1 km using NCAR's REORDER (Oye et al. 1995).

Particle identification (PID) was performed using the polarimetric information from ARMOR. NCAR's PID algorithm was utilized and tuned for C-band (Vivekanandan et al. 1999, Deierling et al. 2008). The primary hydrometeor type and property observed is the volume of graupel within the mixed phase region (-10°C to -40°C) where electrification is known to occur.

Multiple Doppler analysis was performed between ARMOR and the Weather Service Radar-88D (WSR-88D) at Hytop, AL (KHTX). In order to retrieve accurate vertical velocities, radar volume times between the two radars were required to occur within 2 minutes of each other. This requirement reduces errors in vertical velocity retrieval. Using NCAR's Custom Editing and Display of Reduced Information in Cartesian Space (CEDRIC; Mohr et al. 1986), dual-Doppler synthesis was performed with a manual input of storm motion. The variational integration technique was used for multi-Doppler synthesis to minimize errors within the retrievals (Matejka and Bartels 1998). This requires that the anelastic continuity equation is integrated from an upper and a lower boundary and vertical motion at these boundaries are set to 0 m s<sup>-1</sup>. Upward integration from the lower boundary condition occurs in the lowest three vertical levels of the grid space, and downward integration from the upper boundary occurs in the remaining vertical levels.

Three dimensional total lightning information was collected by the NASA's North Alabama Lightning Mapping Array (NALMA, Koshak et al. 2004, Goodman et al. 2005). NALMA is a 11 station array operating between 76-82 MHz that is centered at the National Space Science and Technology Center on the campus of the University of Alabama-Huntsville. The peak power of very high frequency (VHF) radiation source points associated with electrical breakdown are collected every 80 μs. These VHF source points are then recombined using a flash clustering algorithm developed by McCaul et al. (2009) to build flashes. A flash must have a minimum of 10 VHF source points to be considered in this analysis.

Thunderstorms examined in this study were objectively tracked using output from the Thunderstorm Identification Tracking Analysis and Nowcasting algorithm (TITAN; Dixon and Wiener 1993). These objective storm tracks provided a framework in which storm based characteristics (e.g., total flash rate, peak reflectivity, graupel volume, etc.) can be recorded with time, analyzed for trends and intercompared with each other for integrated, multi-platform storm analysis.

Lightning jumps were objectively identified using the 2σ algorithm from Schultz et al. (2009; 2011). This technique uses 14 minutes of the thunderstorm's recent flash rate history to understand if the current behavior of a storm's flash rate is abnormal. As outlined in Schultz et al. (2009, 2011), the algorithm is a 5 step process.

- 1) The total flash rate from the 14 minute period is binned into 2 minute time periods, and the total flash rate is averaged.
- 2) The time rate of change of the total flash rate (DFRDT) is calculated by subtracting consecutive bins from each other (i.e., bin<sub>2</sub>-bin<sub>1</sub>, bin<sub>3</sub>-bin<sub>2</sub>,... bin<sub>7</sub>-bin<sub>6</sub>). This results in 6 DFRDT values with the units of flashes min<sup>-2</sup>.

- 3) Next the 5 oldest values are used to calculate a standard deviation of the population. Twice this standard deviation value determines the jump threshold.
- 4) If the remaining newest DFRDT time exceeds the jump threshold, a jump has occurred. A jump ends once DFRDT drops below 0 flashes  $\text{min}^{-2}$  as new data are collected.
- 5) This process is repeated every two minutes as new total lightning flash rates are collected until the storm dissipates.

In order for a jump to be valid, the total flash rate must exceed 10 flashes per minute. This threshold is used to mitigate smaller jumps in total lightning that commonly occur in ordinary convective storms (i.e., non-severe).

The convective morphology of storms within this study includes isolated ordinary storms, multicellular convection, supercells (including tropical and low echo centroid storms), and quasi-linear convective systems (QLCS). The purpose behind examining this spectrum of storms is to understand not only the physics and kinematics of severe storms, but also to understand what typically occurs in ordinary convection. A total of 18 events, with over 30 individual storms are used in this study; however, for this specific paper, only 4 lightning jumps will be discussed in detail.

## RESULTS

The following observations presented are from four jumps during which multiple Doppler, polarimetric and 3D total lightning coverage were all available. These four events include a pulse severe hailstorm, non-tornadic supercell, a QLCS that produces copious amounts of large hail, and a typical multicellular severe storm that produces wind damage during the summer months. Three of these jumps occur during the development stages of the severe convection (multicell, supercell, QLCS) while the fourth occurs after the convection has already matured.

### *May 3, 2006*

Data from this analysis was originally presented in Johnson (2009). Thunderstorms developed along the remnant of a decaying cold front stalled over the Lower Tennessee Valley during the afternoon of May 3, 2006. At 2130 UTC, a storm developed along this boundary in Madison Co. AL and drifted southward. An objectively identified  $2\sigma$  lightning jump occurred with this storm at 2144 UTC, as the total flash rate increases from 6 flashes  $\text{min}^{-1}$  at 2142 UTC to 19 flashes  $\text{min}^{-1}$  at 2144 UTC (Fig. 3a). During the 8 minutes prior to this lightning jump, the  $10 \text{ m s}^{-1}$  updraft volume exploded from  $8 \text{ km}^3$  to  $202 \text{ km}^3$  while the  $15 \text{ m s}^{-1}$  updraft volume went from not existing within the storm to a volume of  $90 \text{ km}^3$  (Fig. 3b). Maximum vertical velocity nearly doubles during this same period, as the peak updraft speed increases from  $12.2 \text{ m s}^{-1}$  to  $27.8 \text{ m s}^{-1}$  (Fig. 3c). Graupel volume also doubled during this period, increasing from  $32 \text{ km}^3$  to  $79 \text{ km}^3$  (Fig. 3d). At 2154 UTC 1.9 cm hail was observed in North Huntsville 10 minutes after the lightning jump.

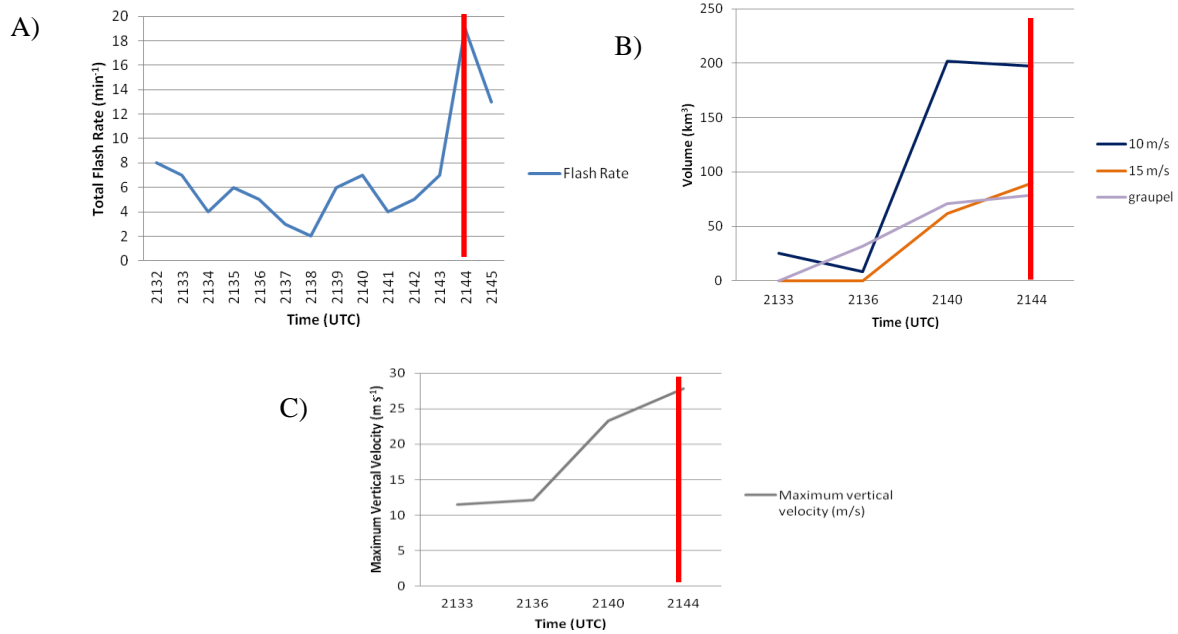


Figure 2. Flash rate, updraft characteristics and graupel volume for a multicellular thunderstorm on May 3, 2006. Panel A) depicts total flash rate vs time, B) 10 and 15 m s<sup>-1</sup> updraft and graupel volume and C) maximum vertical velocity during the previous 11 minutes leading up to the lightning jump. The lightning jump is denoted by the red vertical bar.

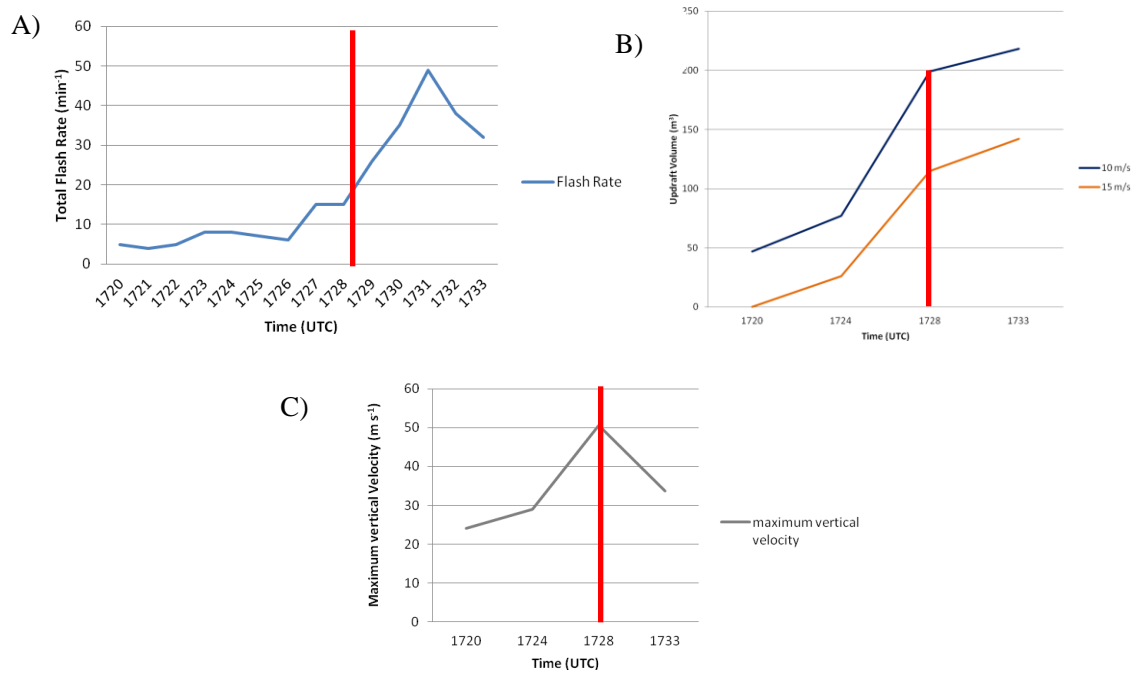


Figure 3. Flash rate, updraft characteristics and graupel volume for a supercell thunderstorm on April 10, 2009. Panel A) depicts total flash rate vs time, B) 10 and 15 m s<sup>-1</sup> updraft and graupel volume and C) maximum vertical velocity during the previous 11 minutes leading up to the lightning jump. The lightning jump is denoted by the red vertical bar.

*April 10, 2009*

A number of supercells pounded the Southeastern US with severe weather on this day. Specifically in the Tennessee Valley, at least 8 supercell storms produced hail to the size of baseballs, and 1 EF3 tornado. The storm examined here did not produce a tornado, but did produce hail up to 1.75 inches in diameter.

The storm specifically studied is ideal for analysis because the first objectively identified  $2\sigma$  lightning jump with this storm occurs at 1728 UTC as it transitioned from a non-severe convective element into a full-fledged supercell. Figure 3 shows total lightning, graupel and updraft volume/speed trends near the time of the objectively identified lightning jump at 1728 UTC. Here the total flash rate explodes from 10 flashes per minute to 40 flashes per minute within a span of 4 minutes (Fig. 3a). During this same period, dual Doppler analysis reveals that the 10 and 15  $\text{m s}^{-1}$  updraft volume also increases dramatically during this period (Fig. 3b).

Figures 4a-d show the 4 dual-Doppler times leading up to and through the lightning jump occurrence. At 1720 UTC the updraft at 6 km is fairly typical for an ordinary (i.e., non-severe) thunderstorm with a

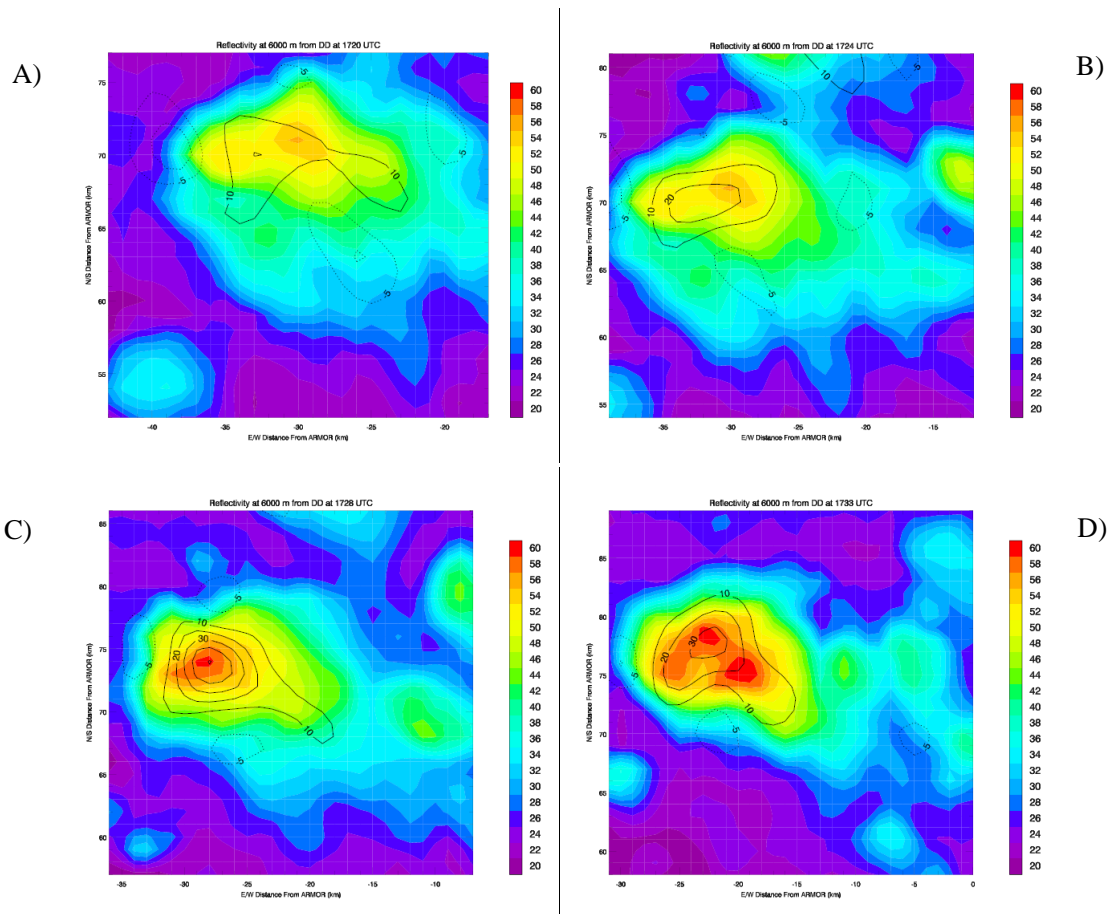


Figure 4.  $Z_{HH}$  and updraft speed at 6 km from ARMOR-KHTX dual-Doppler analysis for four time periods leading up to and through the lightning jump time (a. 1720 UTC, b. 1724 UTC, c. 1728 UTC, d. 1733 UTC).

peak magnitude just over  $10 \text{ m s}^{-1}$  (Fig. 4a). By 1724 UTC, the peak updraft magnitude has increased significantly within the mixed phase region, now just over  $20 \text{ m s}^{-1}$  (Fig. 4b). By 1728 UTC the updraft has increased again by a factor of 2 to over  $40 \text{ m s}^{-1}$  (Fig. 4c) and maintains its strength through 1733 UTC (Fig. 4d). These four panels also indicate that  $Z_{\text{HH}}$  has also increased at this level during the same time period, which corresponds with the theory that an increase in precipitation-sized ice within the mix phase region enhanced charging and ultimately lightning production (e.g., Carey et al. 2000, Deierling et al. 2008). Furthermore, the storm's mesocyclone developed immediately after the lightning jump (Stough et al. 2014), and a lightning hole was present 5 minutes after the lightning jump (Kozlowski and Carey 2014).

**March 12, 2010**

A QLCS on the morning of March 12, 2010 produced copious amounts of hail and high winds across Marshall, Jackson and Dekalb Counties in Alabama. Damage included many trees down, windows blown out and holes in siding from hail being driven into the sides of homes. The portion of the QLCS responsible for the damaging wind and hail swath intensified as it entered the ARMOR-KHTX dual-Doppler domain at 1500 UTC.

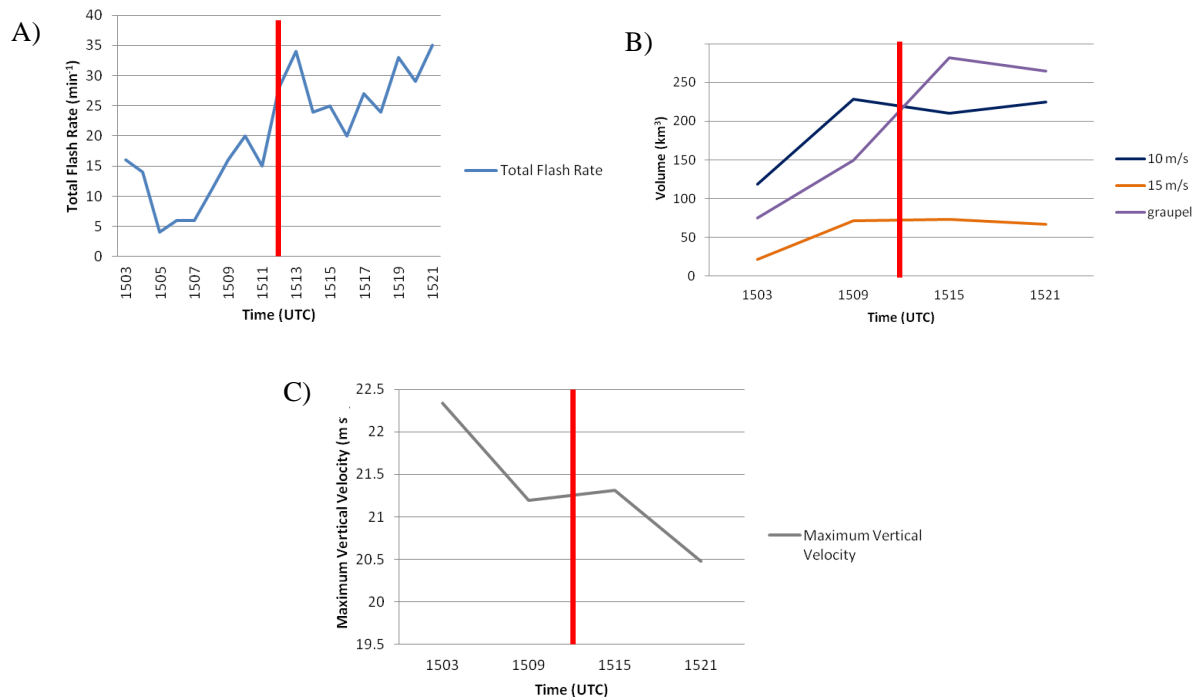


Figure 5. Flash rate, updraft characteristics and graupel volume for the severe portion of a QLCS on March 12, 2010. Panel A) depicts total flash rate vs time, B) 10 and 15  $\text{m s}^{-1}$  updraft and graupel volume and C) maximum vertical velocity during the previous 11 minutes leading up to the lightning jump. The lightning jump is denoted by the red vertical bar.

The first  $2\sigma$  lightning jump occurred within the damaging portion of the QLCS occurred at 1512 UTC. Here the total flash rate increased from 16 flashes per minute to 35 flashes per minute in two minutes (Fig. 5a). Updraft volumes also spiked during this period from  $119 \text{ km}^3$  to  $228 \text{ km}^3$  for  $10 \text{ m s}^{-1}$  updraft volume and  $21 \text{ km}^3$  to  $71 \text{ km}^3$  for  $15 \text{ m s}^{-1}$  updraft volume (Fig. 5b). Also seen in Fig. 5b is the spike in inferred graupel volume within the mixed phase region ( $-10^\circ\text{C}$  to  $-40^\circ\text{C}$ ) near the time of the lightning jump. Graupel volume increased dramatically, from  $75 \text{ km}^3$  at 1503 UTC to  $282 \text{ km}^3$  by 1515 UTC. Interestingly, the maximum updraft speed did not increase, but remained steady between 1503 and 1515 UTC, with a value of  $21 \text{ m s}^{-1}$  (Fig. 5c).

It is unclear at this point the exact reasoning why the peak updraft remained constant and did not increase during the period leading up to the jump like in Figs. 3b and 4b, and further interrogation of the storm is necessary. However, the lack of an increase in the peak updraft at the time of the lightning jump is not surprising because the particles responsible for charge separation have typical fall speeds less than  $5\text{-}10 \text{ m s}^{-1}$ . Thus, within a region of peak updraft (e.g.,  $> 20 \text{ m s}^{-1}$ ) graupel and ice hydrometeors necessary for electrification have shorter residence times that inhibit precipitation growth and charging from rebounding collisions between riming graupel and cloud ice (e.g., MacGorman et al. 2008, Kozlowski and Carey 2014). Updraft volumes (e.g.,  $10$  or  $15 \text{ m s}^{-1}$ ) have more control on the ability for the storm to levitate because fall speeds of the precipitation ice-sized particles needed to facilitate development of a strong electric field capable for electrical breakdown are similar, allowing for longer residence times. This hypothesis is also corroborated by previous studies that show that peak updraft speed is not always well correlated with the total flash rate (e.g., Kuhlman et al. 2006, Deierling et al. 2008).

Two additional jumps were observed within this section of the QLCS at 1550 UTC and 1602 UTC (not shown). Numerous hail reports between 0.75-1.75 inches were reported across Northeast AL between 1500-1700 UTC and the amount of hail was so great that hail remained on the ground for several hours after the event.

## **July 19, 2006**

The thunderstorms on the afternoon of July 19, 2006 were fairly typical for the summer time across the Southeast US, where the main threat from the strongest storms of the day would be high winds. The multicellular thunderstorm examined here developed near Fayetteville, TN, and eventually produced wind damage within city limits. Unfortunately, the volumetric coverage from ARMOR was not available for the first two lightning jumps associated with this storm, however, ARMOR began scanning the storm at 2041 UTC, just prior to the observance of a third jump and subsequent severe weather.

At 2041 UTC when ARMOR volumetric scans began on the storm, the peak flash rate was already at 44 flashes per minute (Fig. 6a). At 2045 UTC the flash rate had increased modestly to 48 flashes per minute; however, by 2050 UTC, the total flash rate had peaked at 65 flashes per minute. A lightning jump occurred in between these two volume times at 2047 UTC.

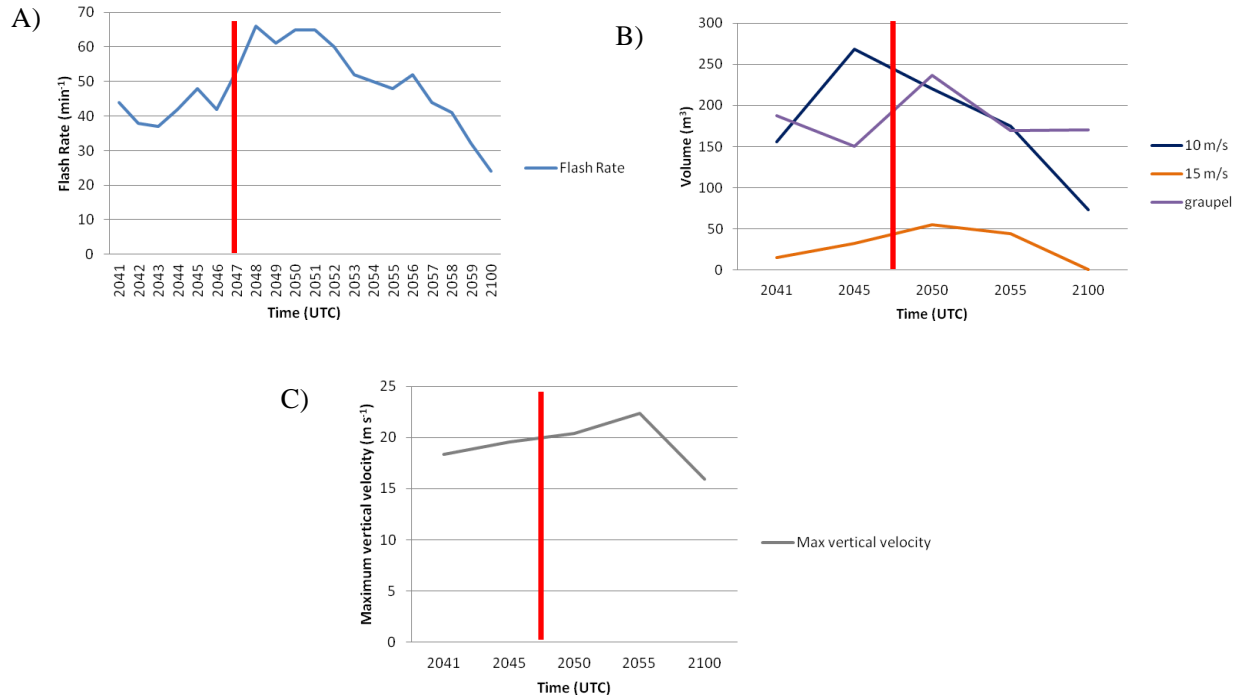


Figure 6. Flash rate, updraft characteristics and graupel volume for a multicellular thunderstorm on July 19, 2006. Panel A) depicts total flash rate vs time, B) 10 and 15 m s<sup>-1</sup> updraft and graupel volume and C) maximum vertical velocity during the previous 11 minutes leading up to the lightning jump. The lightning jump is denoted by the red vertical bar.

Similar behavior in updraft volume was observed to the previous three cases in which the first lightning jumps with those storms were analyzed. Figure 6b shows that both 10 and 15 m s<sup>-1</sup> updraft volumes increased leading up to the jump time at 2047 UTC. Here 10 m s<sup>-1</sup> updraft volume increases from 156 km<sup>3</sup> at 2041 UTC to 268 km<sup>3</sup> at 2045 UTC. Similarly, 15 m s<sup>-1</sup> updraft volume increased from 15 km<sup>3</sup> at 2041 UTC to 32 km<sup>3</sup> at 2045 UTC, eventually peaking at 51 km<sup>3</sup> at 2050 UTC. Unlike the March 12, 2010 case, graupel volume fell from 188 km<sup>3</sup> to 150 km<sup>3</sup> between 2041 and 2045 UTC before increasing once again at 2050 UTC to 237 km<sup>3</sup>. Finally, maximum updraft speed remained steady at 20 m s<sup>-1</sup> leading up to and through the lightning jump (Fig. 6c). Importantly, this final jump occurred prior to the manifestation of damaging winds at the surface that were observed between 2050 and 2108 UTC.

## CONCLUSIONS

The results presented above highlight the following observations at the time of the lightning jumps analyzed:

- 1) Increases in 10 and 15 m s<sup>-1</sup> updraft volume are observed leading up to the time of the lightning jump on a variety of severe thunderstorm types (pulse, multicell, QLCS, supercell).

- 2) Maximum velocity does not always increase in magnitude leading up to the jump, and can remain steady in magnitude or even decrease slightly. This observation is important to note because while updraft speed provides information on the largest particle size that can be lofted, it is the updraft volume that controls the amount of precipitation and the residence of hydrometeors within the storm. Thus, the amount of precipitation lofted relates to precipitation loading leading to an increased potential for severe convective winds and particle residence time is a key factor in hail growth.
- 3) Graupel volume is shown to increase dramatically with the total flash rate, but can lag the increase in updraft volume.

Currently, examination of non-lightning jump producing storms is being completed to compare with cases that contain objectively identified lightning jumps using  $2\sigma$ , and other large increases in total lightning that may not be classified as objective lightning jumps (e.g.,  $> 5$  flashes  $\text{min}^{-2}$ ) in order to fully understand the physical relevance of the  $2\sigma$  lightning jump algorithm. Ongoing work also continues to quantify relationships between lightning jumps and other intensity metrics such as Maximum Expected Size of Hail (MESH; Witt et al. 1998) and azimuthal shear (e.g., Smith and Elmore 2004) using an expanded dataset from Schultz et al. (2011), with the overall goal of providing probabilistic information on storm intensity based on physical and kinematic relationships. Additional information on the relationships between lightning jumps, MESH and azimuthal shear can be found in Schultz et al. (2014; this conference) and Stough et al. (2014; this conference).

## REFERENCES

- Bringi, V. N., T. D. Keenan, V., Chandrasekar, 2001: Correcting C-Band radar reflectivity and differential reflectivity data for rain attenuation: A self-consistent method with constraints. *IEEE Trans. on Geo. and Rem. Sens.*, **39**, 1906-1915.
- Carey, L. D. and S. A. Rutledge, 2000: On the relationship between precipitation and lightning in tropical island convection: A C-band polarimetric radar study. *Mon. Wea. Rev.*, **128**, 2687-2710.
- Chronis, T. and Coauthors, 2014: National Demonstration and Evaluation of a Real Time Lightning Jump Algorithm for Operational Use. *Preprints 26<sup>th</sup> Conf. on Wea. Analysis and Forecasting*, Atlanta, GA. Amer. Met. Soc.
- Deierling, W., W. A. Petersen, J. Latham, S. Ellis, and H. J. Christian, 2008: The relationship between lightning activity and ice fluxes in thunderstorms. *J. Geophys. Res.*, **113**, D15210, doi:10.1029/2007JD009700.
- Deierling, W. and W. A. Petersen, 2008: Total lightning activity as an indicator of updraft characteristics. *J. Geophys. Res.*, **113**, doi:10.1029/2007JD009598.

- Gatlin, P. N. and S. J. Goodman, 2010: A total lightning trending algorithm to identify severe thunderstorms. *J. Atmos. Oceanic Technol.*, **27**, 3-22.
- Goodman, S. J. and Coauthors, 2005: The North Alabama Lightning Mapping Array: Recent severe storm observations and future prospects. *Atmos. Res.*, **76**, 423-437.
- Goodman, S. J., and Coauthors, 2013: The GOES-R Geostationary Lightning Mapper (GLM). *Atmos. Res.*, **125-126**, 34-49.
- Johnson, E. V., 2009: Behavior of Lightning and Updrafts for Severe and Non Severe Thunderstorms in Northern Alabama. M.S. Thesis, University of Alabama-Huntsville, 70 pp.
- Koshak, W. J. and Coauthors, 2004: North Alabama Lightning Mapping Array (LMA): VHF source retrieval algorithm and error analysis. *J. Atmos. Ocean. Tech.*, **21**, 543-558.
- Kozlowski, D. M., and L. D. Carey, 2014: An Analysis of Lightning Holes in Northern Alabama Severe Storms Using a Lightning Mapping Array and Dual-Polarization Radar. *Preprints 5<sup>th</sup> ILMC*, Tuscon, AZ. Vaisala.
- Knupp, K. R., and Coauthors, 2014: Meteorological Overview of the Devastating 27 April 2011 Tornado Outbreak. *Bull. Amer. Meteorol. Soc.*, in press, doi: <http://dx.doi.org/10.1175/BAMS-D-11-00229.1>
- Kuhlman, K. M., C. L. Ziegler, E. R. Mansell, D. R. MacGorman, and J. M. Straka, 2006: Numerically simulated electrification and lightning of the 29 June STEPS supercell storm. *Mon. Wea. Rev.*, **134**, 2734-2757.
- MacGorman and Coauthors (2008), TELEX: The Thunderstorm Electrification and Lightning Experiment. *Bull. Amer. Meteor. Soc.*, **89**, 997-1013.
- McCaul, E. W, Jr., S. J. Goodman, K. M. LaCasse, and D. J. Cecil, 2009: Forecasting lightning threat using cloud-resolving model simulations. *Wea. Forecasting*, **24**, 709-729.
- Matejka, T. and D. L. Bartels, 1998: The accuracy of vertical air velocities from Doppler radar data. *Mon. Wea. Rev.*, **92**, 92-117.
- Mohr, C. G., L. J. Miller, R. L. Vaughn, and H. W. Frank, 1986: The merger of mesoscale data sets into a common Cartesian format for efficient and systematic analysis. *J. Atmos. Ocean. Technol.*, **3**, 143-161.
- Oye, D. and M. Case, 1995: REORDER: A program for Gridding Radar Data. Installation and User

Manual for the UNIX Version. NCAR Atmospheric Technology Division, Boulder, CO, 19 pp.

- Schultz, C. J., W. A. Petersen, and L. D. Carey, 2009: Preliminary development and evaluation of lightning jump algorithms for the real-time detection of severe weather. *J. Appl. Meteor.*, **48**, doi:10.1175/2009JAMC2237.1.
- Schultz, C. J., W. A. Petersen, and L. D. Carey, 2011: Lightning and severe weather: A comparison between total and cloud-to-ground lightning trends. *Wea. and Forecasting*, **26**, 744-755, doi:10.1175/WAF-D-10-05026.1.
- Schultz, C. J. and Coauthors, 2012a: Dual-polarization tornadic debris signatures Part I: Examples and utility in an operational setting. *Electronic J. Operational Meteor.*, **13**, 120-137.
- Schultz, E. V. and Coauthors, 2014: Enhanced Verification of the lightning jump algorithm. *Conference Proceedings 15<sup>th</sup> International Conf. on Atmospheric Electricity*. Norman, OK.
- Smith, T. and K. Elmore, 2004: The use of radial velocity derivatives to diagnose rotation and divergence. Preprints, 11th Conf. on Aviation, Range, and Aerospace, Hyannis, MA, Amer. Meteor. Soc., CD-ROM, P5.6.
- Stough, S. M., L. D. Carey and C. J. Schultz, 2014: Total lightning as an indicator of mesocyclone behavior. *Conference Proceedings 15<sup>th</sup> International Conf. on Atmospheric Electricity*. Norman, OK.
- Straka, J. M., D. S. Zrnich, and A. V. Ryzhkov, 2000: Bulk hydrometeor classification and quantification using polarimetric radar data: Synthesis of relations. *J. Appl. Meteorol.*, **39**, 1341-1372.
- Vivekanandan, J., D. S. Zrnich, S. M. Ellis, R. Oye, A. V. Ryzhkov, and J. Straka, 1999: Cloud microphysics retrieval using S-band dual-polarization radar measurements. *Bull. Amer. Meteorol. Soc.*, **80**, 381-388.
- Williams, E. R. and Coauthors, 1999: The behavior of total lightning activity in severe Florida thunderstorms. *Atmos. Res.*, **51**, 245-265.
- Witt, A., M. D. Eilts, G. J. Stumpf, E. D. Mitchell, J. T. Johnson, and K. W. Thomas, 1998: Evaluating the performance of WSR-88D severe storm detection algorithms. *Wea. and Forecasting*, **13**, 513-518.